Available online at www.sciencedirect.com
SCIENCE DIRECT®
Journal of Organometallic Chemistry 689 (2004) 4384–4394
Journal of Organometallic Chemistry
www.elsevier.com/locate/jorganchem

Transition metal clusters and supported species with metal–carbon bonds from first-principles quantum chemistry

Konstantin M. Neyman [a], Georgi N. Vayssilov [b], Notker Rösch [c,*]

[a] Departament de Química Física, Institució Catalana de Recerca i Estudis Avançats (ICREA), Universitat de Barcelona, 08028 Barcelona, Spain
[b] Faculty of Chemistry, University of Sofia, 1126 Sofia, Bulgaria
[c] Department Chemie, Technische Universität München, 85747 Garching, Germany

Received 8 April 2004
Available online 30 July 2004

Abstract

We discuss the impact of density functional electronic structure calculations for understanding the organometallic chemistry of transition metal (TM) surface complexes and clusters. Examples will cover three types of systems, mainly of interest in the context of heterogeneous catalysis: (i) supported carbonyl complexes of rhenium on MgO and of rhodium in zeolites, (ii) TM clusters with CO ligands and adsorbates, and (iii) metal clusters exhibiting chemical bonds with atomic carbon. The first group of case studies promotes the concept that surface groups of oxide supports are bonded to TM complexes in the same way as common (poly-dentate) ligands are bonded in coordination compounds. The second group of examples demonstrates various "ligand effects" of TM clusters. Finally, we illustrate how carbido centers stabilize TM clusters and modify the propensity for adsorption at the surface of such clusters.

Keywords: Density functional calculations; Transition metal complexes; Transition metal clusters; Heterogenous catalysis; Metal–carbon bonds

1. Introduction

High-level quantum chemistry calculations of organometallic complexes, mainly based on density functional (DF) methods [1–3], turned out to be an inherent part of the research in organometallic chemistry since more than a decade [4–6]. Considerable interest in organometallic compounds derives from their relevance to *homogeneous* catalysis. Recent striking developments in both computer hardware and software for electronic structure calculations made it possible to expand notably the scope of theoretical applications beyond classical organometallic compounds and reactions. For instance, significantly more complicated systems featuring metal–carbon bonds, such as organometallic species anchored on various supports and nanosize metal clusters either with organometallic ligands or containing interstitial/adsorbed carbon atoms or both, are becoming more routinely accessible to first-principles theoretical studies performed with adequate models. The systems just mentioned are of importance for *heterogeneous* catalysis.

Thus, while the role of quantum chemistry methods by now is well established in the theory of organometallic chemistry pertinent to homogeneous catalysis [7], we would like to illustrate new research opportunities that today are offered by electronic structure calculations on organometallic aspects of heterogenous catalysis. We will do so by highlighting certain issues of transition metal (TM) clusters and surface complexes rather than attempting a comprehensive account of this multifarious and rapidly developing field. The interested reader can find a broader coverage of some pertinent issues in

* Corresponding author. Tel.: +49-89-289-13620; fax: +49-89-289-13622.
E-mail address: roesch@ch.tum.de (N. Rösch).

0022-328X/$ - see front matter © 2004 Elsevier B.V. All rights reserved.
doi:10.1016/j.jorganchem.2004.06.042

recent review articles [8–11]. Here, we will focus on conceptually important results that contributed to moving the frontier and making a lasting change. In this spirit, we selected the three groups of representative case studies, both very recent ones and older works that pioneered computational chemistry in this area.

The first group (Section 2) includes supported carbonyl complexes of rhenium on magnesium oxide [12] and those of rhodium encapsulated in zeolite cavities [13,14]. These investigations illustrate how high-level quantum chemistry calculations, in combination with spectroscopic methods, enable one to determine structure and location of organometallic complexes anchored at oxide supports. Furthermore, these works substantiated the concept that an adsorption site, consisting of surface groups of an oxide supports, binds to a TM complex in essentially the same way as common multi-dentate ligands are bonded in coordination compounds.

The second group of examples (Section 3) focuses on TM clusters with CO ligands and adsorbates. An important conceptual aspect is how a non-zero magnetic moment of some bare metal clusters is affected by the presence of ligands [15,16]. Another issue of significant practical importance is whether the vibrational fingerprint of probe CO molecules adsorbed on very small supported metal particles correlates with the charge state of these particles [17,18]. CO probes adsorbed on nanosize clusters also illustrate the advantages of recently suggested three-dimensional models of metal surfaces and supported catalysts. These new types of metal cluster models allow one to reproduce reliably a wide range adsorption parameters, including the very sensitive adsorption energy [19–21]. At the same time, these nanosized metal clusters permit one to clarify the conceptually important issue how different ligand–metal bonding in metal clusters differs from molecular adsorption at metal surfaces and for which sizes of metal particles these differences may became negligible.

Finally, with the third group of examples (Section 4), we discuss complications in the structure and properties of metal clusters which are introduced by bonds formed with atomic carbon, either as species occupying interstitial positions between metal centers [22,23] or as adsorbed surface/subsurface impurity [24]. In particular, we will demonstrate very recent progress in outlining how carbon impurities affect the stability of clusters and how they modify the propensity of clusters to adsorb molecules or interact with a support.

Most of the computational studies discussed in the following were performed with the LCGTO-FF-DF (linear combination of Gaussian-type orbitals fitting-function density functional) method [2] as implemented in the parallel computer code PARAGAUSS [25,26]. Extended systems were represented throughout by cluster models [27]. Unless specified otherwise, the exchange-correlation (XC) functionals VWN [28] and BP86 [29,30] were used to carry out DF calculations in the local-density (LDA) and generalized-gradient (GGA) approximations, respectively. Relativistic effects in systems containing atoms of 4d and 5d elements were accounted for at the scalar relativistic level [31].

2. Supported metal–carbonyl complexes

2.1. $Re(CO)_3$ species on MgO Surface

Supported organometallic species are invaluable for industrial catalysis [32]. However, only very few of them usually form structurally uniform surface complexes and therefore their unequivocal characterization at the atomic level is notably impeded.

Rhenium subcarbonyls on MgO are among the best-studied organometallic complexes on oxides [33,34]. Extended X-ray absorption fine structure (EXAFS) [33] and infrared (IR) spectroscopy [34] data demonstrated that the decomposition of carbonyl precursors on MgO powder results in fragments, assigned as $Re(CO)_3^{n+}$, which are coordinated to the surface. Structural models of the supported complexes have been put forward that represent various degrees of surface hydroxylation, ranging from $Re(CO)_3\{OMg\}_3$, where the metal moiety interacts with three oxygen anions of MgO, to $Re(CO)_3\{HOMg\}_3$, where the fragment interacts with three surface hydroxyl groups of MgO [33,34]. From the positions of the IR bands in the fundamental carbonyl region, the average number of surface oxide and hydroxide moieties coordinated to a Re atom of the supported complexes was estimated [34]. Based on vibrational spectroscopy fingerprints, two limiting complexes were assigned to C_{3v} symmetry [34], implying a surface site with three oxygen atoms involved. No further structural insight could be obtained solely based on the spectroscopic data.

A DF GGA investigation was decisive for determining the structure of these adsorbed species [12]. At the same time, this study was one of the first to assess quantitatively structure and bonding parameters of oxide-supported organometallic species at a reliable computational level. The spectroscopic results suggested that supported $Re(CO)_3$/MgO complexes were located at cationic defects (V_s centers, i.e. Mg vacancies), but the oxidation state of the metal center as well as of the defect site were unknown as was the local degree of hydroxylation. Therefore, a range of models was examined in that study [12]: moieties $Re(CO)_3$ of Re(0) and $Re(CO)_3^+$ of Re(I) on neutral and charged cationic defects V_s, V_s^- and V_s^{2-} centers of dehydroxylated as well as hydrohylated corner sites of MgO surface. Fig. 1 shows sketches of the models and summarizes the main computational results.

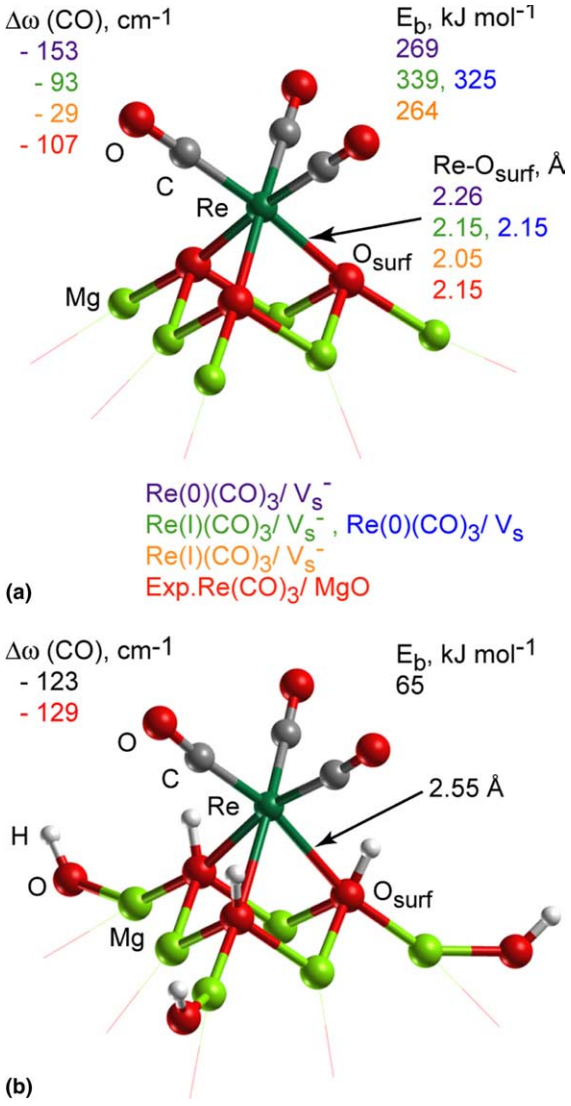

Fig. 1. Sketches of adsorption complexes of rhenium tricarbonyl species on (a) dehydroxylated $Re(CO)_3\{OMg\}_3$ and (b) hydroxylated $Re(CO)_3\{HOMg\}_3$ cationic defects at corner sites of MgO. Also shown are calculated and experimental $Re–O_{surf}$ distances, C–O vibrational frequency shifts $\Delta\omega$ with respect to free molecules, and adsorption energies E_b per $Re–O_{surf}$ bond.

It was found that the structures of the supported complexes $Re(CO)_3\{OMg\}_3$ and $Re(CO)_3\{HOMg\}_3$, proposed on the basis of spectroscopic results, indeed correspond to stable configurations of the investigated cluster models. The computed geometric and vibrational spectroscopy parameters of the dehydroxylated complexes $Re(I)(CO)_3/V_s^-$ and $Re(0)(CO)_3/V_s$ ($\Delta\omega(CO) = -93$ cm^{-1}) as well as of the hydroxylated complex $Re(I)(CO)_3/V_s(OH)$ ($\Delta\omega(CO) = -123$ cm^{-1}) have been obtained in qualitative agreement with experiment (-107 and -129 cm^{-1}, respectively), thus complementing available experimental information and validating the structural models.

Furthermore, the assumption that the adsorbate–substrate interactions weakened with increasing surface hydroxylation, inferred from the IR C–O frequency shift [34], was corroborated and rendered more precise by calculated adsorption energies. In fact, surface hydroxylation was found to reduce dramatically the adsorption energy (per $Re–O_{surf}$ bond) from 339 to 65 kJ mol^{-1}. This finding implies possibilities for tuning adsorptive and catalytic properties of supported organometallic species by modifying the surface stoichiometry even of such an inert oxide support as MgO.

Another very noteworthy computational result is that the $Re–O_{surf}$ bonds of supported complexes $Re(CO)_3\{OMg\}_3$ on V_s and V_s^- defects are really similar in nature and strength (260–340 kJ mol^{-1}) to common coordination bonds. Even stronger adsorption interactions of various mononuclear subcarbonyl products of decarbaonlyated $Re_2(CO)_{10}$ on γ-alumina (basically restricted to only one $Re–O_{surf}$ bond formed) have been found in a nonrelativistic DF study [35] employing the hybrid XC functional B3PW91. These observations justify the concept of *surface sites acting as (poly-dentate) ligands* which are able to anchor organometallic fragments to supports.

2.2. Mononuclear Rh carbonyl species in zeolite cavities

The well-defined crystalline structure of zeolites provides an opportunity for much more ordered and uniform location of transition metal species and complexes compared to the metal oxide or silica support surface [36]. However, location and structure of such adsorption complexes cannot be determined based on the available experimental techniques alone and high-level quantum chemical calculations contribute crucially to validate such knowledge. We illustrate a combination approach, relying on spectroscopic and computational information, for the example of cationic rhodium dicarbonyl complex embedded in the cavities of dealuminated Y zeolite (DAY) [13]. This type of materials features two very sharp IR bands of CO symmetric and antisymmetric modes that confirms the formation of dicarbonyls and implies uniform location and structure of $Rh(CO)_2^+$ species in zeolite [37]. The EXAFS measurements verify that the observed species are mononuclear rhodium complexes and they provide a reference for bonding distances and the number of oxygen atoms bound to a rhodium cation. Yet, EXAFS data cannot directly determine the location of the complex in zeolite cavities; in fact, the obtained spectra could be rationalized with three different models corresponding to different numbers of O ligands from the zeolite. However, the complex was identified with the help of a series of DF model calculations that checked which of the suggested adsorption complexes inside zeolite fits best the experimental characteristics obtained by EXAFS and IR spectroscopy. The computationally derived structure is planar with a rhodium cation bound to two zeolite

oxygen centers and both CO ligands oriented along the continuation of Rh–O_{zeo} bonds (Fig. 2(a)); Fig. 2(b) shows how the species are located in the supercage of DAY zeolite. The correspondence between EXAFS derived and DF calculated bond distances is very good [13]; values differs at most by 4 pm for the nearest neighbors and by 7 pm for the next-nearest neighbors. The difference in the infrared CO frequency shifts of the adsorbed species with respect to gas phase CO molecule is also small, 4–11 cm^{-1}.

With the clarification of the location of $Rh(CO)_2^+$ species in DAY zeolite, it became possible to determine also the structure of less stable rhodium carbonyl species in zeolite and to assign their IR frequencies [14]. Using the same computational approach and structural models, we examined the assignment of the experimentally observed weak IR band at 2093 cm^{-1} assumed to correspond to $Rh(CO)^+$ species [37,38]. Our simulations suggested that this band should be assigned to rhodium carbonyl species which contain additional hydrogen ligands, e.g. $Rh(CO)(H_2)^+$ or $Rh(CO)(H)_2^+$, whereas the zeolite supported complex $Rh(CO)^+$ is characterized by the IR band observed at 2014 cm^{-1} [37], with a frequency shift relative to dicarbonyl similar to the experimental IR shift of the corresponding molecular Rh^+ carbonyl complexes [39].

A similar strategy, combining spectroscopic and computational information, was recently applied successfully to study nickel (II) monocarbonyl [40] and dicarbonyl [41] complexes grafted onto tridentate silica support.

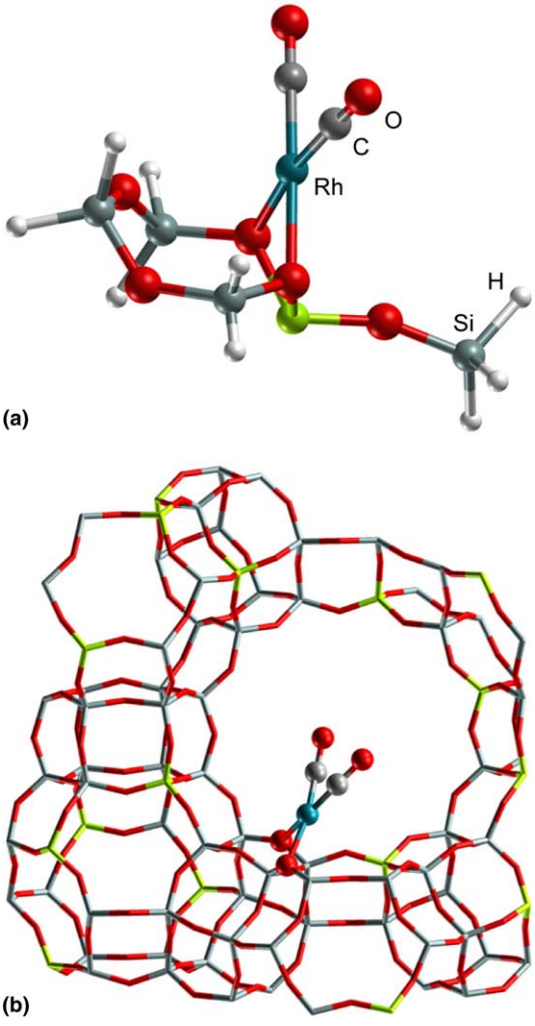

Fig. 2. Structure of the cationic rhodium dicarbonyl complex inside DAY zeolite (a) determined by a combination of DF calculations, IR, and EXASF measurements and (b) sketch showing the location of the species inside a zeolite cavity.

3. Transition metal clusters with carbonyl ligands and adsorbates

3.1. Effect on the cluster magnetism

Molecular ligands at TM clusters affect the structure, electron distribution, and other electronic and magnetic properties of the clusters [15,16,42]. Whereas bare nickel clusters are magnetic [43–46], coordination of CO ligands leads to a reduction the magnetism or even to a complete quenching if all metal atoms are coordinated by a sufficient number of ligands, e.g. $[Ni_6(CO)_{12}]^{2-}$ or $[Ni_{48}Pt_6(CO)_{12}]^{n-}$. This ligand-induced change of the magnetic moment can be rationalized by an analysis of the orbital occupation in bare and ligated TM clusters. Bare TM clusters exhibit a magnetic moment when the $(n–1)$d manifold of the metal atoms is not completely filled, e.g. in nickel clusters at the expense of a partially filled ns level manifold. Coordination of the CO ligands to the metal atoms is accompanied by a repulsive interaction of the CO 5σ lone pair orbital with the extended orbitals of the TM ns level manifold. Simultaneously, back-donation occurs from filled $(n-1)$d orbitals of the metal with the $2\pi^*$ antibonding MO of CO. When CO ligands approach a metal cluster, cluster orbitals of mainly ns character are destabilized first due to Pauli repulsion because the spatial extension of ns-derived levels is much larger than that of metal orbitals of the $(n-1)$d manifold [15]. Due to this repulsion, ns levels of the metal are shifted above the Fermi level [15,47] and the corresponding electrons end up in $(n-1)$d orbitals; as a result, the open-shell character of the nd manifold is reduced and the magnetic moment is partially or completely quenched. This electron redistribution on the metal atoms of the cluster entails formation of Me–C bonds according to the well-known donation-back donation mechanism. The Me–CO interaction is bonding only when such electron redistribution occurs from filled ns to empty $(n-1)$d orbitals; it is repulsive if the redistribution is restricted and the ns orbitals remain filled [16].

As example for the electronic interaction in a TM carbonyl cluster we present in Fig. 3 the density of states (DOS) of the cluster $Ni_6(CO)_{12}^{2-}$. The 5σ lone pair orbitals of the CO ligands are considerably stabilized and not shown in the figure. Due to the interaction with the 2π* orbitals of CO, the 3d manifold of Ni is stabilized below Fermi level ε_F, whereas the antibonding 2π* orbitals of the CO ligands destabilized, and a substantial HOMO–LUMO gap of more than 1 eV is formed. In agreement with the discussion above, one can clearly see that the Ni 4s manifold is pushed higher in energy, in part even above the CO 2π* partial DOS.

Larger clusters which comprise more than one shell of Ni atoms have been shown to retain some of their magnetism, because the effect of CO ligand attachment is localized essentially to the TM atoms in the surface of the cluster [15,16,48].

3.2. Probing the charge of supported metal particles by adsorbed CO

Chemical bonds of probe CO molecules on various surfaces contain valuable information on both the morphology and electronic state of the adsorption sites under investigation. For adsorption complexes of CO with metal oxide and zeolite substrates, part of this information can be conveniently extracted by examining the frequency alteration of the fundamental carbonyl vibration measured by IR spectroscopy [36,49]. In similar fashion, CO can be utilized to probe the charge (oxidation) state and the interfacial coordination chemistry of TM species grafted on oxide surfaces or in zeolites. Organometallic complexes with metal–carbon bonds formed in these latter cases enable one to bridge the gap between organic and coordination chemistry [50]. Electronic structure calculations often provide indispensable reference data for quantifying the charge state of supported or encaged TM particles via examination of parameters of adsorbed CO probes.

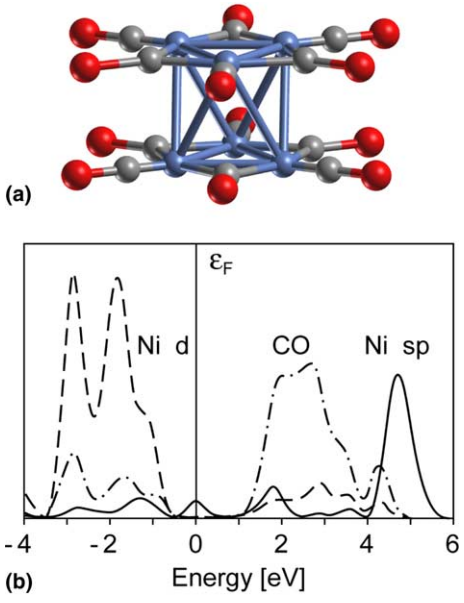

Fig. 3. Sketch of (a) the cluster $[Ni_6(CO)_{12}]^{2-}$ and (b) its calculated density of states.

Based on experimental data, very small TM species, stabilized inside zeolite cavities, have been proposed to exhibit electron enriched and electron deficient states [51]. As an example for the value of computational studies of this aspect, we mention DF investigations of the cluster Pt_4, in both neutral and electronically modified form [17]. The species Pt_4^+ has been chosen to represent a metal particle interacting with an electron attracting zeolite host; likewise, Pt_4^- has been taken to model the effect of an electron donating host. Adsorption of CO probe molecules at on-top, bridge, and threefold hollow sites of the moieties Pt_4, Pt_4^+, and Pt_4^- has been studied to determine a relationship between the cluster charge and the C–O vibrational frequency shift $\Delta\omega$(CO). Furthermore, the chemical effect of electron–donor and electron–acceptor species on the electronic structure of Pt_4 clusters and on adsorbed CO probes has explicitly been accounted in the models XPt_4CO (X = Na, Na^+, NH_3). In line with experimental evidence, adsorbed CO probe molecules were calculated to be rather sensitive to the electronic state and the adsorption site of the Pt_4 particles. Finally, a linear correlation between the effective charge of the metal cluster and the adsorption-induced vibrational frequency shift $\Delta\omega$(CO) was found for CO adsorbed at on-top positions.

An IR band with very low frequency, $\Delta\omega(CO) = -186\ cm^{-1}$, has been measured for terminal CO molecules on Pt_n species formed by decomposing the Chini complex $[Pt_3(CO)_3(\mu\text{-}CO)_3]_3^{2-}$ in NaX zeolite [52]. That frequency shift was attributed to a negative charge of the encapsulated platinum cluster, in good agreement with the above mentioned correlation [17]. Note that combination of DF results [53] and vibrational spectroscopy data for CO adsorption complexes with Pt species in mordenite, assigned to be as small as monatomic moieties [54] turned out to be electron-deficient.

A more sophisticated DF study [18] explicitly addressed the interaction of an Ir_4 cluster with a zeolite support, represented by a ring consisting of six O atoms and six T (Si or Al) atoms facing the supercage of a faujasite framework (Fig. 4). Changes in the electronic structure of the metal cluster with respect to a free cluster were again probed via bonding of a CO molecule to the supported Ir_4 species at the on-top site. Careful analysis of the C–O vibrational frequency, calibrated against the charge borne by the bare Ir_4 cluster, showed that the interaction of the cluster with the zeolite induces electron donation *from the support to the cluster*, notable

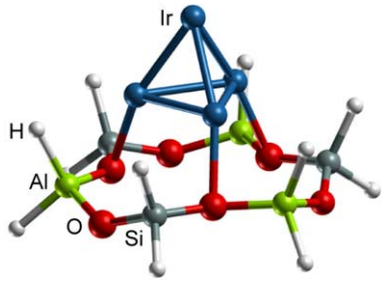

Fig. 4. Most stable configuration of the cluster Ir_4 supported on the zeolite six-ring fragment $[Al_3Si_3O_6H_{12}]^{3-}$.

through a somewhat enhanced red-shift of the C–O stretching frequency. This conceptually noteworthy result can probably be generalized for other small *ligand-free* TM clusters interacting mainly with basic oxygen atoms of zeolite and metal-oxide supports: provided that such supported metal clusters can be stabilized, they are expected to either be essentially zero-valent or acquire a negative charge.

This assumption, namely stabilization of ligand-free TM clusters in zeolites (and on other oxide supports) under ambient conditions after decarbonylation of a precursor TM cluster compound, has also been questioned in that combined examination of calculated DF and measured EXAFS results [18]. For supported Ir_4, the metal–metal distance was calculated at about 250 pm, only a few pm longer than in a free Ir_4 cluster, but about 20 pm shorter than derived by EXAFS for various zeolite-supported clusters assigned as Ir_4. The EXAFS distances characterizing the zeolite-supported clusters are very similar to calculated and measured values for the coordinatively saturated cluster compound $Ir_4(CO)_{12}$ which, in turn, is similar to the nearest-neighbor distance of bulk Ir metal. This finding suggested that the supported clusters, investigated with EXAFS spectroscopy, were not entirely ligand free: at variance with earlier assumptions, their formation by decarbonylation of the parent $Ir_4(CO)_{12}$ did not proceed by simple, complete removal of all CO ligands. This very important conclusion is not unexpected in the light of the relatively weak interaction, calculated for small ligand free metal clusters on oxide support [8,9], so that they have to be classified as essentially unsaturated and highly reactive. On the other hand, the optimized structure of an unsupported model clusters Ir_4 with a single C atom as ligand matches the EXAFS Ir–Ir distance, thus favoring the hypothesis of a carbon impurity on zeolite-supported clusters [18]. Very recently, for a well-characterized zeolite-supported Rh_6 cluster, a computational study demonstrated that also reverse hydrogen spill-over from hydroxyl groups of the zeolite framework may induce metal–metal distances that are close to those of the corresponding bulk metal [55,56].

3.3. CO adsorption on nanosize clusters modeling metal surfaces and supported catalysts

Now, we turn from TM carbonyl cluster compounds, as they typically occur in cluster chemistry, to computational studies of adsorption systems with organometallic bonds formed by CO molecules with notably larger TM clusters. Such nanosize clusters with more than 50 atoms are important for various reasons. For instance, as recently demonstrated for the first time [19], with three-dimensional nanocluster models one can reach cluster size convergence for many chemical properties, even including the adsorption energy on a metal surface – an observable that is very sensitive to cluster size. Furthermore, such models [19–21] bring important insight into the theoretical description of adsorption properties and the reactivity of so-called supported model catalysts which are notably less complex than industrial metal catalysts on oxides [57,58].

Probe CO molecules at the (1 1 1) single-crystal surface of Pd form typical surface organometallic bonds [59]. Theoretical studies of such adsorption interactions on metals are often based on the model cluster approach [27], which allows one to accurately reproduce a variety of observables. However, adsorption energies usually show considerable variations with size and shape of the cluster models [60,61].

To reach convergence, it was recently proposed to use cluster models comprising of up to more than hundred atoms, but terminated by low-index crystal planes [19]; these ‘‘nanocrystal’’ models can be chosen to exhibit sufficiently large point group symmetry, with great computational advantage. A series of octahedral clusters Pd_{55}–Pd_{146}, with the geometry fixed as in Pd bulk, have been calculated, focusing on the interaction of CO with the threefold hollow sites on (1 1 1) facets of the clusters. For this series of cluster models, it was examined how different adsorption parameters vary with cluster size and how these values of cluster models relate to adsorption properties of the corresponding site at the single crystal surface Pd(1 1 1). Starting from Pd_{79}, the calculations for the substrate models [19] yielded adsorption energies per CO molecule which varied in a narrow interval of 5 kJ mol^{-1}. Thus, nanoscale models of about 80 Pd atoms no longer exhibit notable size effects for the properties of adsorption complexes. This very important finding indicates that convergence of adsorption energies on a TM single-crystal surface can be reached with moderately large compact cluster models, terminated by low-index crystal facets. Such models avoid the drawbacks of conventional cluster models where too many metal atoms at the boundaries are insufficiently coordinated [27] and they appear to represent the polarizability of a metal surface with sufficient accuracy. Furthermore, the adsorption energy of CO from ‘‘converged’’ cluster models is essentially in *quantitative*

agreement with energies calculated from periodic slab models, provided the same XC functional is used in both calculations [19].

The calculated harmonic frequency ω(C–O) ~ 1755 cm^{-1} [19] is about 4% smaller than the value of 1825 cm^{-1} measured at low CO coverage on Pd(1 1 1) [62]. Such a frequency underestimation is common for contemporary GGA XC functionals for bonds involving a TM atom [63]. When the bonds under scrutiny are not very weak, LDA geometries and vibrational frequencies are often more accurate than GGA values; gradient-corrected functionals often appear to "improve" *only* binding energies [63]. For systems such as CO/Pd featuring organometallic bonds with heavy d-metal atoms, an XC functional, that accurately represents *both* geometric observables *and* energetics, is still to be constructed.

Carbon monoxide is not only a touchstone adsorbate but also a key reagent in industrial syntheses over oxide-supported TM catalysts [32]. For this reason, the adsorption of CO on nanosize Pd particles was studied theoretically and spectroscopically, by means of infrared reflection absorption spectroscopy (IRAS) and sum frequency generation (SFG) [20]. A DF approach was applied to three-dimensional crystallites of about 140 Pd atoms. The model clusters were chosen as octahedral fragments of the fcc bulk, exhibiting (1 1 1) and (0 0 1) facets. Various types of adsorption sites were probed by CO: threefold hollow, bridge, and on-top positions at (1 1 1) facets; fourfold hollow and on-top sites at (0 0 1) facets; bridge positions at cluster edges; on-top positions at cluster corners and on single Pd atoms deposited at regular (1 1 1) facets. For a summary of selected calculated results, see Fig. 5 [20]. Adsorption properties of the relatively small regular cluster facets (1 1 1) and (0 0 1) were calculated similar to those of an infinite (1 1 1) Pd surface. However, the strongest CO bonding was calculated for bridge positions at cluster edges. The energy of adsorption on-top of low-coordinated Pd centers (kinks) was also calculated larger than that for on-top sites of (1 1 1) and (0 0 1) facets.

In that combined spectroscopic and computational study [20], vibrational spectra of CO adsorbed on supported Pd nanocrystallites of different size and structure (well-faceted and defect-rich) were measured using IRAS and SFG and correlated with the theoretical results. For CO adsorption under UHV conditions, a characteristic absorption in the frequency region 1950–1970 cm^{-1} was observed, which in agreement with the theoretical data were assigned to vibrations of bridge-bonded CO at particles edges and defects. Based on these calculated data, it was possible to interpret the experimentally observed differences in CO adsorption on alumina-supported Pd nanoparticles of different size and surface quality [20]. That study convincingly demonstrated the power of modern dedicated theoretical tools based on DF schemes. In combination with sophisticated spectroscopic experiments, modern computational chemistry is able to provide insights into structure and properties of complex materials, such as model supported TM catalysts, and molecular surface complexes featuring organometallic bonds.

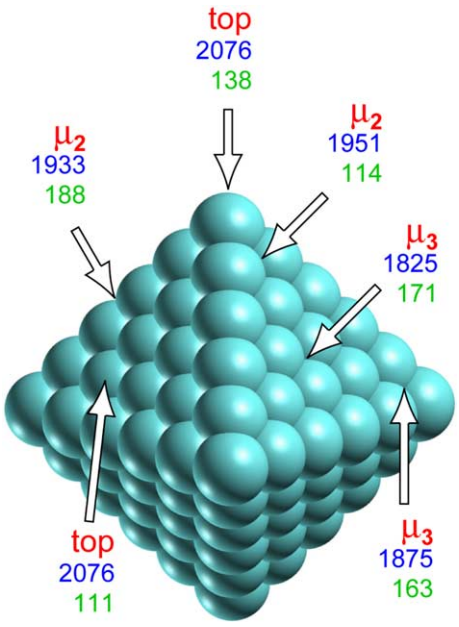

Fig. 5. Calculated DF GGA adsorption energies E_b(Pd–CO) (kJ mol^{-1}) and vibrational frequencies ω(C–O) (cm^{-1}) of CO molecules adsorbed on various sites of Pd_{146}.

Bimetallic nanoparticles are even more complex – thus, more challenging for an accurate theoretical description – than monometallic species as just addressed. Nevertheless, we were able to report very recently a first DF investigation of the active component of novel Pd/ZnO catalysts for methanol steam reforming [21]. Focusing on systems with low Zn concentrations, we studied a series of isostructural bimetallic cuboctahedral nanoclusters Pd_{140}, $Pd_{132}Zn_8$(0,8), $Pd_{116}Zn_{24}$(24,0), $Pd_{108}Zn_{32}$(24,8), and $Pd_{116}Zn_{24}$(0,24) as local models of the catalysts [21]. (Here, the numbers of Zn atoms in the surface and sub-surface layers, respectively, are given in parentheses; see Fig. 6 for example structures.) The calculated average cluster cohesive energy was found to decrease gradually with increasing number of Zn atoms: each Zn atom destabilizes the cluster by ~100 kJ mol^{-1}. CO probe molecules adsorbed at hollow Pd_3 sites of the (1 1 1) cluster facets (Fig. 6(a)), were used to explore how the adsorption properties of bimetallic species change with respect to those of the reference cluster Pd_{140} [19]. Calculated CO adsorption energies manifest a weakening of the adsorbate–substrate organometallic bonds when Zn atoms are located in the subsurface layer of the $Pd_{140-n}Zn_n$ clusters; however, Zn atoms in the surface layer affect the CO adsorption energy only marginally. No correlation was found between calculated CO adsorption energies and

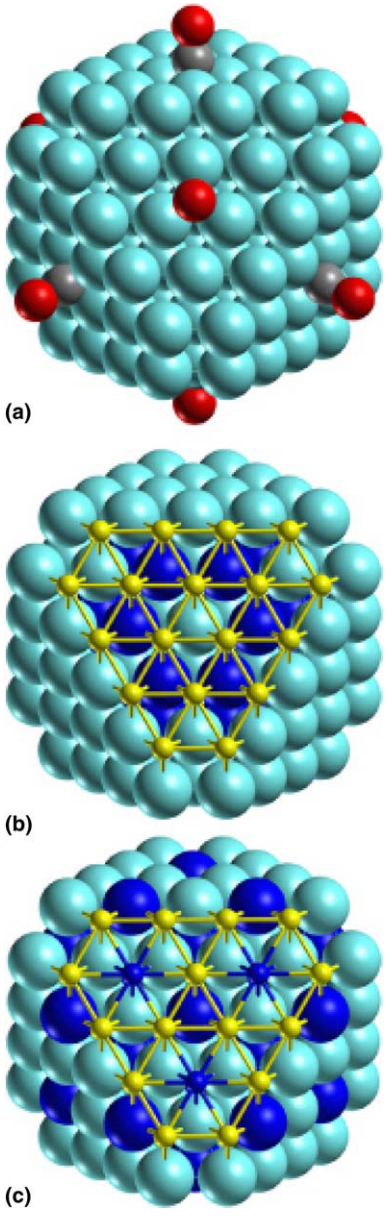

Fig. 6. Sketches of cuboctahedral nanoclusters: (a) representative adsorption complex $Pd_{140}(CO)_8$; (b) $Pd_{108}Zn_{32}$(24,8), (c) $Pd_{116}Zn_{24}$-(0,24). In parentheses are the numbers of Zn atoms in the surface and sub-surface layers, respectively. For clarity, the first layer of one (1 1 1) facet in panel b is depicted as a network of bonds only.

vibrational C–O frequencies. This was traced back to the different nature of these properties: binding energies are *global* characteristics of adsorption systems whereas vibrational frequencies are mainly determined by the *local* environment of a site.

4. Bonding of atomic carbon with metal clusters

Thus far, we discussed systems featuring conventional organometallic TM–carbon bonds. However, other TM–carbon interactions, namely those involving atomic C species, are also of immediate interest for both organometallic chemistry and heterogeneous catalysis by metals. For instance, interstitial atomic carbon species (among other main-group elements) are known to be often present in the metal core of metal cluster compounds (see [15] and references therein). Furthermore, atomic carbon moieties can be generated during catalytic transformations of organic molecules and deposited on TM particles as impurities, affecting the performance of a catalyst or even poisoning it [64]. In the following, we will exemplify theoretical efforts to rationalize structure and properties of transition and noble metal clusters containing atomic carbon.

4.1. Carbon centered clusters

Already in the beginning of the past decade, metal cluster compounds with interstitial C atoms attracted close attention of theoretical chemists working with the first-principles methods. As an example, we mention a series of LDA calculations of nickel carbonyl clusters [15,65]. At that time, even such complicated systems as octahedral main-group element centered gold cluster compounds, featuring strong relativistic effects, became accessible to accurate DF calculations [22]. It is worth recalling the conclusions of relativistic LDA investigations regarding the central atom in the touchstone cluster $\{[(R_3P)Au]_6C\}^{2+}$ [22]. First, C and Au orbitals interact directly, stabilizing each other. Second, a formal transfer of four electrons occurs from the fragment $[(H_3P)Au]_6^{2+}$ into the C 2p orbitals which, together with radial C–Au bonds, contributes to the stability of the cluster compound due to electrostatic interaction between the negatively charged central C atom and the positively charged Au_6 shell.

A decade later, computational studies of much more complex systems with carbon-centered polynuclear metal particles became possible. As an example, we mention a DF GGA study of an Os_5C cluster supported on regular sites and V_s and V_s^{2-} defects of a MgO(0 0 1) surface [23]. These models were chosen because small clusters on MgO formed after complete decarbonylation of supported $[Os_5C(CO)_{14}]^{2-}$ show, according to EXAFS measurements [66], retention of the metal frame, including a carbido C atom. The interaction of a Os_5C cluster with the support was calculated to range from very weak ($\sim$60 kJ mol^{-1}) at regular sites when basal Os atoms are aligned with the nearest O_{surf} anions, via moderately strong ($\sim$170 kJ mol^{-1}) at V_s^{2-} defect sites, to rather strong ($\sim$470 kJ mol^{-1}) at neutral V_s defects. Os–Os bond distances were calculated to be about 30–50 pm shorter than the values measured by EXAFS spectroscopy – far outside the bounds of the generally accepted inaccuracy of DF methods [3]. As discussed above for other small TM clusters formed by decarbonylation of metal carbonyl cluster precursors (see Section 3.2), this

finding indicated that the Os_5C clusters supported on MgO powder are likely not entirely free of ligands or other atomic impurities. The most plausible model of TM clusters supported on powder MgO includes light-atom ligands that are formed during decarbonylation; they remain virtually undetectable with EXAFS and are difficult to identify also by other spectroscopic techniques.

4.2. Carbon impurities on Pd nanoparticles: adsorption and diffusion subsurface

One should expect that TM-C bonds in carbon-centered clusters, as just addressed, and in TM nanoclusters with atomic carbon impurities occupying surface or subsurface/bulk positions are very similar. A very recent DF GGA study [24] dealt with surface/subsurface carbon (and other light atoms) impurities in Pd nanoclusters; it also considered the effect of such impurities on the adsorption properties manifested by carbonyl probe molecules adsorbed above subsurface impurities.

For this purpose, models were investigated with single carbon atoms adsorbed at threefold hollow sites in the center of each of the eight hexagonal (1 1 1) facets of the cuboctahedral clusters Pd_{79} and Pd_{116} (Fig. 7) [24]. For the cluster Pd_{79}, the carbon atoms were also allowed to "migrate" from their fcc surface hollow sites to the interstitial octahedral (tetrahedral) hole sites underneath; similarly, migration of carbon to subsurface hcp hole sites was modeled with the cluster Pd_{116}. These models provided insight into the relative stability of surface and subsurface carbon species as well as the activation barriers for migration from surface to subsurface positions. Structural relaxation of the Pd substrates was accounted for, while O_h symmetry constraints were maintained for computational efficiency.

The calculations showed that subsurface carbon species occupying octahedral holes below the surface threefold fcc sites of the cluster Pd_{79} are almost isoenergetic with adsorption complexes at fcc surface sites, with binding energies E_b of 677 and 663 kJ mol^{-1}, respectively [24]; these very strongly bound impurities bear significant negative charge of about $-1e$. The calculations yielded a moderate activation barrier of $\sim$60 kJ mol^{-1} for diffusion of atomic carbon species from surface fcc sites to octahedral subsurface sites. On the other hand, carbon impurities in tetrahedral subsurface positions of the cluster Pd_{116} (E_b = 559 kJ mol^{-1}) were calculated to be energetically disfavored relative to adsorption at hcp sites at the cluster surface (E_b = 676 kJ mol^{-1}).

The presence of subsurface carbido species in octahedral holes significantly decreases the energy of CO adsorption at surface sites directly above the impurities, from 156 to 81 kJ mol^{-1}; this reduction of binding energies can be mainly attributed to a local oxidation of Pd centers by atomic carbon [24]. By the same token, the C–O vibrational frequency of CO molecules adsorbed above subsurface C impurities in Pd_{79} nanoclusters, 1831 cm^{-1}, is notably larger than the stretching frequencies computed on a structurally optimized carbon-free cluster, 1755 cm^{-1} [24], and estimated within the same computational approach for threefold hollow sites of a clean Pd(1 1 1) surface, $\sim$1750 cm^{-1} [19].

Currently, this study of carbon impurities is extended by examining the diffusion between various regular sites and surface irregularities of palladium nanoclusters [67].

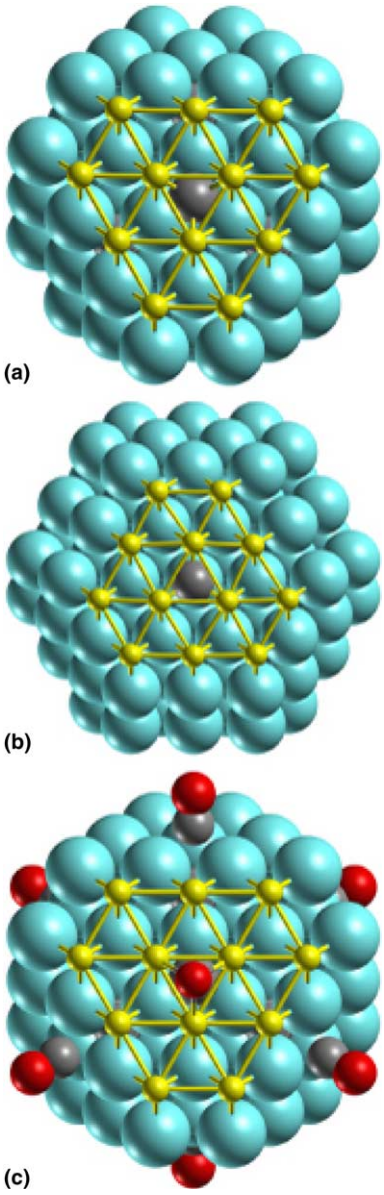

Fig. 7. Cuboctahedral palladium nanoclusters with subsurface atomic carbon species under each of their eight (1 1 1) facets: (a) $Pd_{116}C_8$ – interstitial C in tetrahedral holes, (b) $Pd_{79}C_8$ – interstitial C in octahedral holes, (c) $Pd_{79}C_8(CO)_8$ – CO adsorbed on fcc sites with subsurface C beneath. For clarity, the first layer of one (1 1 1) facet is depicted as a network of bonds only.

5. Conclusions and outlook

We provided a brief account of the research opportunities offered by modern high-level DF electronic structure methods to address a variety of organometallic chemistry problems of transition metal surface complexes and clusters, mainly of interest in the context of heterogeneous catalysis. As examples we selected recent and older DF case studies related to the following three issues: (i) supported carbonyl complexes of rhenium on MgO and of rhodium in zeolites, (ii) TM clusters with CO ligands and adsorbates, and (iii) metal clusters exhibiting chemical bonds with atomic carbon.

The first group of examples illustrated convincingly the power of studies, which combine quantum chemical and spectroscopic studies for determining structure and location of organometallic complexes anchored on oxides. These examples also promoted the concept that surface groups of oxide supports are bonded to TM complexes in the same way as common (poly-dentate) ligands are bonded in coordination compounds.

The second group of examples demonstrated various "ligand effects" of TM clusters, e.g. how ligands affect the magnetic moments of TM clusters, that the vibrational fingerprint of adsorbed probe CO molecules correlates with the charge of these clusters, and which advantages the recently suggested three-dimensional nanocrystallites entail for modeling metal surfaces and supported catalysts.

Finally, the third group of examples, addressing carbon atoms in either interstitial positions between metal centers or as surface/subsurface impurities of TM clusters, showed how carbido centers stabilize TM clusters and modify the propensity for adsorption at the surface of such clusters.

Most of the DF studies reviewed here dealt with adsorption properties. In the future, we can certainly expect an increasing number of computational studies devoted to quantifying the supported subnano- and nanoparticles featuring organometallic bonds. As first examples, we discussed the decarbonylation of $Re_2(CO)_{10}$ over γ-alumina [35] and the kinetics of surface/subsurface diffusion of atomic carbon impurities on Pd nanoclusters [24]. The synthesis of size-selected supported transition and noble metal clusters [68] and the amazing experimental study of reactions performed on such well-characterized systems will undoubtedly stimulate theoretical chemistry contributions. Finally, we would like to mention two recent combined computational and experimental reactivity studies on size-selected metal clusters, on acetylene trimerization over subnanoscale Pd species supported on MgO [69] and on CO oxidation by supported gold nanoparticles [70]. These studies are harbingers of even more fascinating computational results on organometallic reactions of supported metal species that we will undoubtedly see very soon.

Acknowledgements

We are grateful to Chan Inntam for assistance with the figures. This work was supported by Deutsche Forschungsgemeinschaft and Fonds der Chemischen Industrie (Germany).

References

[1] J.C. Slater, The Self-Consistent Field for Molecules and Solids: Quantum Theory of Molecules and Solids, vol. 4, McGraw-Hill, New York, 1974.
[2] B.I. Dunlap, N. Rösch, Adv. Quant. Chem. 21 (1990) 317.
[3] W. Koch, M.C. Holthausen, A Chemist's Guide to Density Functional Theory, Wiley–VCH, Weinheim, 2000.
[4] T. Ziegler, Chem. Rev. 91 (1991) 651.
[5] A. Veillard, Chem. Rev. 91 (1991) 743.
[6] G. Frenking, N. Frohlich, Chem. Rev. 100 (2000) 717.
[7] F. Maseras, A. Lledos (Eds.), Computational Homogeneous Catalysis, Kluwer Academic Publishers, Dordrecht, 2002.
[8] N. Rösch, G.N. Vayssilov, K.M. Neyman, in: F. Laeri, F. Schüth, U. Simon, M. Wark (Eds.), Host–Guest-Systems Based on Nanoporous Crystals, Wiley–VCH, Weinheim, 2003, p. 339.
[9] N. Rösch, V.A. Nasluzov, K.M. Neyman, G. Pacchioni, G.N. Vayssilov, in: J. Leszczynski (Ed.), Computational Material Science, Theoretical and Computational Chemistry Series, Elsevier, Amsterdam, 2004, p. 365.
[10] F. Illas, C. Sousa, J.R.B. Gomes, A. Clotet, J.M. Ricart, in: M.A.C. Nascimento (Ed.), Theoretical Aspects of Heterogeneous Catalysis, Kluwer Academic Publishers, Dordrecht, 2001, p. 149.
[11] J. Greeley, J.K. Nørskov, M. Mavrikakis, Annu. Rev. Phys. Chem. 53 (2002) 319.
[12] A. Hu, K.M. Neyman, M. Staufer, T. Belling, B.C. Gates, N. Rösch, J. Am. Chem. Soc. 121 (1999) 4522.
[13] J.F. Goellner, B.C. Gates, G.N. Vayssilov, N. Rösch, J. Am. Chem. Soc. 122 (2000) 8056.
[14] G.N. Vayssilov, N. Rösch, J. Am. Chem. Soc. 124 (2002) 3783.
[15] G. Pacchioni, N. Rösch, Acc. Chem. Res. 28 (1995) 390.
[16] G. Pacchioni, S. Krüger, N. Rösch, in: P. Braunstein, L.A. Oro, P.R. Raithby (Eds.), Metal Clusters in Chemistry, Wiley–VCH, Weinheim, 1999, p. 1392.
[17] A.M. Ferrari, K.M. Neyman, T. Belling, M. Mayer, N. Rösch, J. Phys. Chem. B 103 (1999) 216.
[18] A.M. Ferrari, K.M. Neyman, M. Mayer, M. Staufer, B.C. Gates, N. Rösch, J. Phys. Chem. B 103 (1999) 5311.
[19] I.V. Yudanov, R. Sahnoun, K.M. Neyman, N. Rösch, J. Chem. Phys. 117 (2002) 9887.
[20] I.V. Yudanov, R. Sahnoun, K.M. Neyman, N. Rösch, J. Hoffmann, S. Schauermann, V. Johánek, H. Unterhalt, G. Rupprechter, J. Libuda, H.-J. Freund, J. Phys. Chem. B 107 (2003) 255.
[21] K.M. Neyman, R. Sahnoun, C. Inntam, S. Hengrasmee, N. Rösch, J. Phys. Chem. B 108 (2004) 5424.
[22] (a) A. Görling, N. Rösch, D.E. Ellis, H. Schmidbaur, Inorg. Chem. 30 (1991) 3986;
(b) O.D. Häberlen, H. Schmidbaur, N. Rösch, J. Am. Chem. Soc. 116 (1994) 8241.
[23] J.F. Goellner, K.M. Neyman, M. Mayer, F. Nörtemann, B.C. Gates, N. Rösch, Langmuir 16 (2000) 2736.

[24] I.V. Yudanov, K.M. Neyman, N. Rösch, Phys. Chem. Chem. Phys. 6 (2004) 116.
[25] T. Belling, T. Grauschopf, S. Krüger, M. Mayer, F. Nörtemann, M. Staufer, C. Zenger, N. Rösch, in: H.-J. Bungartz, F. Durst, C. Zenger (Eds.), High Performance Scientific and Engineering Computing, Lecture Notes in Computational Science and Engineering, vol. 8, Springer, Heidelberg, 1999, p. 439.
[26] T.Belling, T.Grauschopf, S.Krüger, F.Nörtemann, M.Staufer, M.Mayer, V.A. Nasluzov, U.Birkenheuer, A. Hu, A.V. Matveev, A.M. Shor, M.S.K. Fuchs-Rohr, K.M. Neyman, D.I. Ganyushin, T. Kerdcharoen, A.Woiterski, N.Rösch, PARAGAUSS, Version 2.2, Technische Universität München, Munich, 2001.
[27] (a) G. Pacchioni, P.S. Bagus, F. Parmigiani (Eds.), Cluster Models for Surface and Bulk Phenomena, NATO ASI Series B, vol. 283, Plenum Press, New York, 1992;
(b) J.L. Whitten, H. Yang, Surf. Sci. Rep. 24 (1996) 59.
[28] S.H. Vosko, L. Wilk, M. Nusair, Can. J. Phys. 58 (1980) 1200.
[29] A.D. Becke, Phys. Rev. A 38 (1988) 3098.
[30] J.P. Perdew, Phys. Rev. B 33 (1986) 8822 erratum, Phys. Rev. B 34 (1986) 7406.
[31] (a) N. Rösch, S. Krüger, M. Mayer, V.A. Nasluzov, in: J. Seminario (Ed.), Recent Developments and Applications of Modern Density Functional Theory, Elsevier, Amsterdam, 1996, p. 497;
(b) N. Rösch, A. Matveev, V.A. Nasluzov, K.M. Neyman, L. Moskaleva, S. Krüger, in: P. Schwerdtfeger (Ed.), Relativistic Electronic Structure Theory. Part II: Applications, Theoretical and Computational Chemistry Series, Elsevier, Amsterdam, 2004, p. 656.
[32] B.C. Gates, Catalytic Chemistry, Wiley–VCH, New York, 1992.
[33] P.S. Kirlin, F.B.M. van Zon, D.C. Koningsberger, B.C. Gates, J. Phys. Chem. 94 (1990) 8439.
[34] C.J. Papile, B.C. Gates, Langmuir 8 (1992) 74.
[35] J. Räty, M. Suvanto, P. Hirva, T.A. Pakkanen, Surf. Sci. 492 (2001) 243.
[36] K.I. Hadjiivanov, G.N. Vayssilov, Adv. Catal. 47 (2002) 307.
[37] H. Miessner, J. Am. Chem. Soc. 116 (1994) 11522.
[38] K. Hadjiivanov, E. Ivanova, L. Dimitrov, H. Knözinger, J. Mol. Struc. 661 (2003) 459.
[39] T.P. Dougherty, W.T. Grubbs, E.J. Heilweil, J. Phys. Chem. 98 (1994) 9396.
[40] D. Costa, G. Martra, M. Che, L. Manceron, M. Kermarec, J. Am. Chem. Soc. 124 (2002) 7210.
[41] G. Martra, S. Coluccia, M. Che, L. Manceron, M. Kermarec, D. Costa, J. Phys. Chem. B 107 (2003) 6096.
[42] H.A. Aleksandrov, G.N. Vayssilov, N. Rösch, J. Phys. Chem. A 108 (2004) 6127.
[43] I.M.L. Billas, A. Chatelain, W.A. de Heer, Science 265 (1994) 1682.
[44] J.A. Alonso, Chem. Rev. 100 (2000) 637.
[45] S. Krüger, T.J. Seemüller, A. Wörndle, N. Rösch, Int. J. Quantum Chem. 80 (2000) 567.
[46] S. Krüger, M. Stener, N. Rösch, J. Chem. Phys. 114 (2001) 5207.
[47] R. Hoffmann, Solids and Surfaces. A Chemist's View of Bonding in Extended Systems, VCH, New York, 1988 p. 74.
[48] D.A. van Leeuwen, J.M. van Ruitenbeek, L.J. de Jongh, A. Ceriotti, G. Pacchioni, G. Longoni, O.D. Häberlen, N. Rösch, Phys. Rev. Lett. 73 (1994) 1432.
[49] H. Knözinger, in: G. Ertl, H. Knözinger, J. Weitkamp (Eds.), Handbook of Heterogeneous Catalysis, vol. 2, Wiley–VCH, Weinheim, 1997, p. 707.
[50] B.C. Gates, Chem. Rev. 95 (1995) 511.
[51] D. Barthomeuf, Catal. Rev. 38 (1996) 521.
[52] A.I. Serykh, O.P. Tkachenko, V.Yu. Borovkov, V.B. Kazansky, M. Beneke, N.I. Jaeger, G. Schulz-Ekloff, Phys. Chem. Chem. Phys. 2 (2000) 5647.
[53] A.L. Yakovlev, K.M. Neyman, G.M. Zhidomirov, N. Rösch, J. Phys. Chem. 100 (1996) 3482.
[54] V.L. Zholobenko, G.-D. Lei, B.T. Carvill, B.A. Lerner, W.M.H. Sachtler, J. Chem. Soc., Faraday Trans. 90 (1994) 233.
[55] G.N. Vayssilov, B.C. Gates, N. Rösch, Angew. Chem. Int. Ed. 42 (2003) 1391.
[56] G.N. Vayssilov, N. Rösch, J. Phys. Chem. B 108 (2004) 180.
[57] M. Bäumer, H.-J. Freund, Prog. Surf. Sci. 61 (1999) 127.
[58] H.-J. Freund, Surf. Sci. 500 (2002) 271.
[59] G.A. Somorjai, Introduction to Surface Chemistry and Catalysis, Wiley, New York, 1994.
[60] G. te Velde, E.J. Baerends, Chem. Phys. 117 (1993) 399.
[61] L.G.M. Pettersson, T. Faxen, Theor. Chim. Acta 85 (1993) 345.
[62] W.K. Kuhn, J. Szanyi, D.W. Goodman, Surf. Sci. 274 (1992) L611.
[63] A. Görling, S.B. Trickey, P. Gisdakis, N. Rösch, in: J. Brown, P. Hofmann (Eds.), Topics in Organometallic Chemistry, vol. 4, Springer, Heidelberg, 1999, p. 109.
[64] S. Schauermann, J. Hoffmann, V. Johánek, J. Hartmann, J. Libuda, H.-J. Freund, Angew. Chem. Int. Ed. 41 (2002) 2532.
[65] (a) G. Pacchioni, N. Rösch, Inorg. Chem. 29 (1990) 2901;
(b) N. Rösch, L. Ackermann, G. Pacchioni, J. Chem. Phys. 95 (1991) 7004;
(c) N. Rösch, L. Ackermann, G. Pacchioni, J. Am. Chem. Soc. 114 (1992) 3549.
[66] L.F. Allard, G.A. Panjabi, S.N. Salvi, B.C. Gates, Nanoletters 2 (2002) 381.
[67] K.M. Neyman, C. Inntam, A.B. Gordienko, N. Rösch, to be published.
[68] S. Abbet, A. Sanchez, U. Heiz, W.-D. Schneider, J. Catal. 198 (2001) 122.
[69] (a) A.M. Ferrari, L. Giordano, G. Pacchioni, S. Abbet, U. Heiz, J. Phys. Chem. B 106 (2002) 3173;
(b) K. Judai, S. Abbet, A.S. Wörz, A.M. Ferrari, L. Giordano, G. Pacchioni, U. Heiz, J. Mol. Catal. A 199 (2003) 103.
[70] H. Häkkinen, W. Abbet, A. Sanchez, U. Heiz, U. Landman, Angew. Chem. Int. Ed. 42 (2003) 1297.